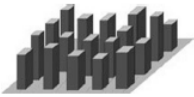




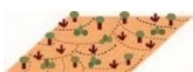






Supplementary Materials: Spatiotemporal Characteristics of the Surface Urban Heat Island and Its Driving Factors Based on Local Climate Zones and Population in Beijing, China

Yatong Zhang ^{1,2}, Delong Li ^{1,2}, Laibao Liu ^{1,2}, Ze Liang ^{1,2}, Jiashu Shen ^{1,2}, Feili Wei ^{1,2} and Shuangcheng Li ^{1,2,*}

Table S1. Local climate zones scheme (Stewart and Oke, 2012).

Built types	Definition	Land cover types	Definition
LCZ 1 Compact high-rise	Dense mix of tall buildings to tens of stories. Few or no trees. Land cover mostly paved. Concrete, steel, stone, and glass construction materials.	LCZ A Dense trees	Heavily wooded landscape of deciduous and/or evergreen trees.
			Land cover mostly pervious (low plants). Zone function is natural forest, tree cultivation, or urban park.
LCZ 2 Compact midrise	Dense mix of midrise buildings (3–9 stories). Few or no trees. Land cover mostly paved. Stone, brick, tile, and concrete construction materials.	LCZ B Scattered trees	Lightly wooded landscape of deciduous and/or evergreen trees.
			Land cover mostly pervious (low plants). Zone function is natural forest, tree cultivation, or urban park.
LCZ 3 Compact low-rise	Dense mix of low-rise buildings (1–3 stories). Few or no trees. Land cover mostly paved. Stone, brick, tile, and concrete construction materials.	LCZ C Bush, scrub	Open arrangement of bushes, shrubs, and short, woody trees.
			Land cover mostly pervious (bare soil or sand). Zone function is natural scrubland or agriculture.
LCZ 4 Open high-rise	Open arrangement of tall buildings to tens of stories. Abundance of pervious land cover (low plants, scattered trees). Concrete, steel, stone, and glass construction materials.	LCZ D Low plants	Featureless landscape of grass or herbaceous plants/crops.
			Few or no trees. Zone function is natural grassland, agriculture, or urban park
LCZ 5 Open midrise	Open arrangement of midrise buildings (3–9 stories). Abundance of pervious land cover (low plants, scattered trees). Concrete,	LCZ E Bare rock or paved	Featureless landscape of rock or paved cover. Few or no trees or plants. Zone function is natural desert (rock) or urban transportation.
			



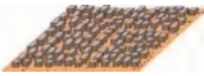




	steel, stone, and glass construction materials.		
LCZ 6 Open low-rise	Open arrangement of low-rise buildings (1–3 stories). Abundance of pervious land cover (low plants, scattered trees). Wood, brick, stone, tile, and concrete construction materials.	LCZ F Bare soil or sand	Featureless landscape of soil or sand cover. Few or no trees or plants. Zone function is natural desert or agriculture.
			
LCZ 7 Lightweight low-rise	Dense mix of single-story buildings. Few or no trees. Land cover mostly hard-packed. Lightweight construction materials (e.g., wood, thatch, corrugated metal).	LCZ G Water	Large, open water bodies such as seas and lakes, or small bodies such as rivers, reservoirs, and lagoons.
			
LCZ 8 Large low-rise	Open arrangement of large low-rise buildings (1–3 stories). Few or no trees. Land cover mostly paved. Steel, concrete, metal, and stone construction materials.		
			
LCZ 9 Sparsely built	Sparse arrangement of small or medium-sized buildings in a natural setting. Abundance of pervious land cover (low plants, scattered trees).		
			
LCZ 10 Heavy industry	Low-rise and midrise industrial structures (towers, tanks, stacks). Few or no trees. Land cover mostly paved or hard-packed. Metal, steel, and concrete construction materials.		
			

Table S2. Regression coefficients for TM\ETM+ and TIRS for different temperature ranges.

Sensor	Temperature ranges (°C)	<i>a</i>	<i>b</i>
TM\ETM+	0~30	-60.3263	0.43436
	20~50	-67.9542	0.45987

TIRS	0~70	-67.35535	0.458608
	0~30	-59.139	0.421
	0~40	-60.919	0.428
	10~40	-62.806	0.434
	10~50	-64.608	0.440

Estimation of emissivity(ϵ)

The emissivity estimation method proposed by Qin et al. (2004) is used in this research. In this method, the land surface is considered being composed by land cover of water, urban surface and nature surface. The emissivity of natural surface is estimated by Equation S1.

$$\epsilon = \begin{cases} P_v R_v \epsilon_v + (1 - P_v) R_s \epsilon_s + d\epsilon, & \epsilon < \epsilon_v \\ \epsilon_v, & \epsilon \geq \epsilon_v \end{cases} \quad (S1)$$

where R_v and R_s are the temperature ratio of vegetation and soil, respectively; P_v is the vegetation fraction calculated by Equation S2 (Carlson and Ripley, 1997); $d\epsilon$ is the contribution of interaction between vegetation and soil on emissivity calculated by formula S3 (Sobrino et al., 2004); ϵ_v and ϵ_s are emissivity of vegetation and soil, respectively.

$$P_v = \begin{cases} 0, & NDVI < NDVI_s \\ \left(\frac{NDVI - NDVI_s}{NDVI_v - NDVI_s} \right)^2, & NDVI_s \leq NDVI \leq NDVI_v \\ 1, & NDVI > NDVI_v \end{cases} \quad (S2)$$

$$d\epsilon = \begin{cases} 0.0038 P_v, & P_v \leq 0.5 \\ 0.0038(1 - P_v), & P_v > 0.5 \\ 0.0019, & P_v = 0.5 \end{cases} \quad (S3)$$

where $NDVI_v$ and $NDVI_s$ are the the Normalized Difference Vegetation Index value of vegetation and soil, respectively. Moreover, the emissivity of urban area was estimated by Equation S4.

$$\epsilon = P_v R_v \epsilon_v + (1 - P_v) R_m \epsilon_m + d\epsilon \quad (S4)$$

where, R_m and ϵ_m are the temperature ratio and emissivity of the built-up surface, respectively.

The R_v , R_s and R_m are calculated by Equation S5–S7 and the value of ϵ_v , ϵ_s , ϵ_m and ϵ_w (the emissivity of water) are listed in Table S3.

$$R_v = 0.9332 + 0.0585 P_v \quad (S5)$$

$$R_s = 0.9902 + 0.1068 P_v \quad (S6)$$

$$R_m = 0.9886 + 0.1287 P_v \quad (S7)$$

Table S3. Emissivity of typical land cover in thermal infrared bands of different sensors.

ϵ_w	ϵ_v	ϵ_s	ϵ_m
--------------	--------------	--------------	--------------

TM\ETM+ band 6	0.995	0.986	0.97215	0.970
TIRS band 10	0.99683	0.98672	0.96767	0.964885

From Qin et al. (2004) and Song et al. (2015)

Estimation of atmospheric transmittance (τ)

Qin et al. (2003) and Rozenstein et al. (2014) proposed the estimation method of atmospheric transmittance of thermal infrared band (band 6 of TM/ETM+ and band 10 of TIRS, Table S4 and Table S5). According to the location of study area and the observation time of Landsat images, the estimation equations was applied with profile condition of high air temperature and water vapor content range of 1.6–3.0 g·cm⁻² (for TM/ETM+ images) and with profile condition of Mid-Latitude Summer (for TIRS).

Table S4. Estimation of the atmospheric transmittance for TM/ETM+.

Profiles	water vapor (ω) (g·cm ⁻²)	Estimation Equation
High air temperature	0.4~1.6	$\tau=0.974290 - 0.08007\omega$
	1.6~3.0	$\tau=1.031412 - 0.11536\omega$
Low air temperature	0.4~1.6	$\tau=0.982007 - 0.09611\omega$
	1.6~3.0	$\tau=1.053710 - 0.14142\omega$

Table S5. Estimation of the atmospheric transmittance for TIRS for the water vapor content range of 0.5~3 g·cm⁻².

Profiles	Estimation Equation
1976US Standard	$\tau= - 0.1146\omega + 1.0286$
Mid-Latitude Summer	$\tau= - 0.1134\omega + 1.0335$

The atmospheric water vapor content can be can be obtained by the conversion of water vapor pressure (Yang and Qiu, 1996):

$$\omega=0.0981e+0.1697 \quad (S8)$$

where e is the water vapor pressure and can be calculated by Equation S9:

$$e = 0.6108 \times \exp\left(\frac{17.27(T_0 - 273)}{237.3 + T_0 - 273}\right) \times RH \times 10 \quad (S9)$$

where T₀ is the air temperature near the surface (K) and RH is the relative humidity (%), which was acquired from meteorological station.

Estimation of average atmospheric temperature (T_a)

According to the method provided by Qin et al. (2003), the average atmospheric temperature (K) can be estimated by the equations listed in Table S6 . The equation for mid-latitude summer was selected in this research.

Table S6. Equations for estimating the average atmospheric temperature.

Standard atmosphere	Equation
USA 1976	$T_a=25.9396+0.88045T_0$
Tropical	$T_a=17.9769+0.91715T_0$
Mid-latitude summer	$T_a=16.0110+0.92621T_0$
Mid-latitude winder	$T_a=19.2704+0.91118T_0$

Table S7. Year matching between distribution maps of LST and LCZ.

LCZ	LST	LCZ	LST
2003	2000	2010	2009

2005	2001	2017	2010
	2002		2011
	2003		2012
	2004		2013
	2005		2014
	2006		2015
	2007		2016
2010	2008		2017

Table S8. Lowest, highest and mean LST (°C) for each LST distribution map.

Year	Lowest	Highest	Mean
2000	6.0	57.8	29.9
2001	14.9	55.4	34.5
2002	4.5	52.9	28.6
2003	6.6	62.4	35.2
2004	23.1	56.0	36.3
2005	24.0	53.8	35.9
2006	12.4	58.6	33.1
2007	12.4	59.5	34.0
2008	18.6	53.3	33.0
2009	10.7	55.6	33.6
2010	15.5	51.4	32.7
2011	7.9	58.6	35.6
2012	13.2	55.3	32.1
2013	5.0	51.5	29.1
2014	16.8	54.1	34.2
2015	18.7	48.2	33.0
2016	16.8	55.2	33.7
2017	20.3	64.5	42.0

Table S9. Confusion matrix of LCZ classification of 2003.

Clas s	LCZ 1	LCZ 2	LCZ 3	LCZ 4	LCZ 5	LCZ 8	LCZ A	LCZ B	LCZ D	LCZ E	LCZ F	LCZ G	SumUser	UA(%)
LCZ 1	80	1	1	12	1	1	0	0	0	6	1	0	103	77.7
LCZ 2	9	69	14	0	1	1	0	0	0	2	0	0	96	71.9
LCZ 3	4	25	178	8	9	0	0	0	0	0	14	0	238	74.8
LCZ 4	30	6	15	212	17	7	3	6	1	18	14	0	329	64.4
LCZ 5	3	22	16	33	244	20	0	7	0	8	4	0	357	68.3
LCZ 8	0	0	0	1	0	144	0	1	0	10	0	0	156	92.3
LCZ A	0	0	0	0	0	0	172	2	8	0	1	0	183	94.0
LCZ B	0	0	0	2	5	1	28	285	31	4	2	2	360	79.2
LCZ D	0	0	0	0	0	0	4	0	243	0	1	0	248	98.0

LCZ E	10	5	2	10	4	8	0	1	0	135	5	0	180	75.0
LCZ F	0	0	0	3	3	1	0	5	20	0	178	0	210	84.8
LCZ G	0	0	0	0	0	0	2	0	0	0	5	261	268	97.4
Σ	136	128	226	281	284	183	209	307	303	183	225	263	Kappa	0.787
PA(%)	58.8	53.9	78.8	75.4	85.9	78.7	82.3	92.8	80.2	73.8	79.1	99.2	OA	0.807

Notes:

UA refers to user's accuracy.

PA refers to producer's accuracy.

OA refers to overall accuracy.

Table S10. Confusion matrix of LCZ classification of 2005.

Clas s	LCZ 1	LCZ 2	LCZ 3	LCZ 4	LCZ 5	LCZ 8	LCZ A	LCZ B	LCZ D	LCZ E	LCZ F	LCZ G	SumUser	UA(%)
LCZ 1	28	0	0	13	0	0	0	0	0	2	0	0	43	65.1
LCZ 2	0	0	0	0	0	0	164	0	80	0	0	7	251	65.3
LCZ 3	0	0	0	0	0	0	15	173	83	0	0	1	272	63.6
LCZ 4	0	0	0	0	0	0	4	1	182	0	0	0	187	97.3
LCZ 5	0	0	78	2	5	24	0	0	0	138	63	0	310	44.5
LCZ 8	0	0	10	0	0	2	0	0	0	0	132	0	144	91.7
LCZ A	2	0	0	0	0	0	1	0	0	0	0	272	275	98.9
LCZ B	3	56	17	0	5	3	0	0	0	20	6	0	110	50.9
LCZ D	0	4	69	0	4	1	0	0	0	8	1	0	87	79.3
LCZ E	4	2	1	237	10	2	0	5	0	7	1	0	269	88.1
LCZ F	3	11	36	10	242	0	0	0	0	28	21	0	351	68.9
LCZ G	1	0	3	0	0	217	0	0	0	0	31	0	252	86.1
Σ	41	73	214	262	266	249	184	179	345	203	255	280	Kappa	0.724
PA(%)	68.3	76.7	32.2	90.5	91.0	87.1	89.1	96.6	52.8	68.0	51.8	97.1	OA	0.749

Notes:

UA refers to user's accuracy.

PA refers to producer's accuracy.

OA refers to overall accuracy.

Table S11. Confusion matrix of LCZ classification of 2010.

Clas s	LCZ 1	LCZ 2	LCZ 3	LCZ 4	LCZ 5	LCZ 8	LCZ A	LCZ B	LCZ D	LCZ E	LCZ F	LCZ G	SumUser	UA(%)
LCZ 1	161	1	22	28	11	0	0	0	0	5	1	14	243	66.3
LCZ 2	8	64	44	1	15	10	0	2	0	17	0	0	161	39.8
LCZ 3	3	9	232	5	34	4	1	0	0	9	1	0	298	77.9
LCZ 4	24	0	11	359	80	0	5	3	0	2	1	10	495	72.5
LCZ 5	4	3	136	44	344	1	2	7	0	4	4	2	551	62.4
LCZ 8	2	9	134	0	2	658	0	0	3	44	2	1	855	77.0
LCZ A	0	0	1	0	4	0	218	29	62	0	0	19	333	65.5
LCZ B	0	0	2	4	9	0	22	63	31	1	1	3	136	46.3

LCZ D	0	1	2	0	0	1	1	15	393	0	2	0	415	94.7
LCZ E	3	5	69	1	11	5	0	0	0	215	5	9	323	66.6
LCZ F	0	7	6	8	0	5	0	5	0	30	209	3	273	76.6
LCZ G	0	0	0	0	0	0	4	0	2	0	0	339	345	98.3
Σ	205	99	659	450	510	684	253	124	491	327	226	400	Kappa	0.706
PA(%)	78.5	64.6	35.2	79.8	67.4	96.2	86.2	50.8	80.0	65.7	92.5	84.8	OA	0.735

Notes:

UA refers to user's accuracy.

PA refers to producer's accuracy.

OA refers to overall accuracy.

Table S12. Confusion matrix of LCZ classification of 2017.

Clas s	LCZ 1	LCZ 2	LCZ 3	LCZ 4	LCZ 5	LCZ 8	LCZ A	LCZ B	LCZ D	LCZ E	LCZ F	LCZ G	SumUser	UA(%)
LCZ 1	138	15	0	35	10	3	0	0	1	3	6	0	211	65.4
LCZ 2	20	129	6	21	3	14	0	0	0	13	14	0	220	58.6
LCZ 3	2	3	496	11	23	27	1	0	0	0	4	2	569	87.2
LCZ 4	41	4	1	535	11	1	3	9	7	3	23	2	640	83.6
LCZ 5	19	2	84	164	456	14	3	2	0	4	1	3	752	60.6
LCZ 8	1	8	12	2	3	362	0	0	0	13	5	1	407	88.9
LCZ A	3	0	0	20	1	1	297	20	41	0	0	0	383	77.5
LCZ B	2	0	0	15	1	0	23	152	54	0	1	0	248	61.3
LCZ D	0	0	0	16	0	6	8	25	306	3	9	0	373	82.0
LCZ E	9	18	24	9	13	26	0	0	3	263	15	0	380	69.2
LCZ F	2	1	4	12	1	10	0	2	6	14	160	0	212	75.5
LCZ G	0	0	0	2	0	0	4	0	0	0	0	453	459	98.7
Σ	237	180	627	842	522	464	339	210	418	316	238	461	Kappa	0.747
PA(%)	58.2	71.7	79.1	63.5	87.4	78.0	87.6	72.4	73.2	83.2	67.2	98.3	OA	0.772

Notes:

UA refers to user's accuracy.

PA refers to producer's accuracy.

OA refers to overall accuracy.

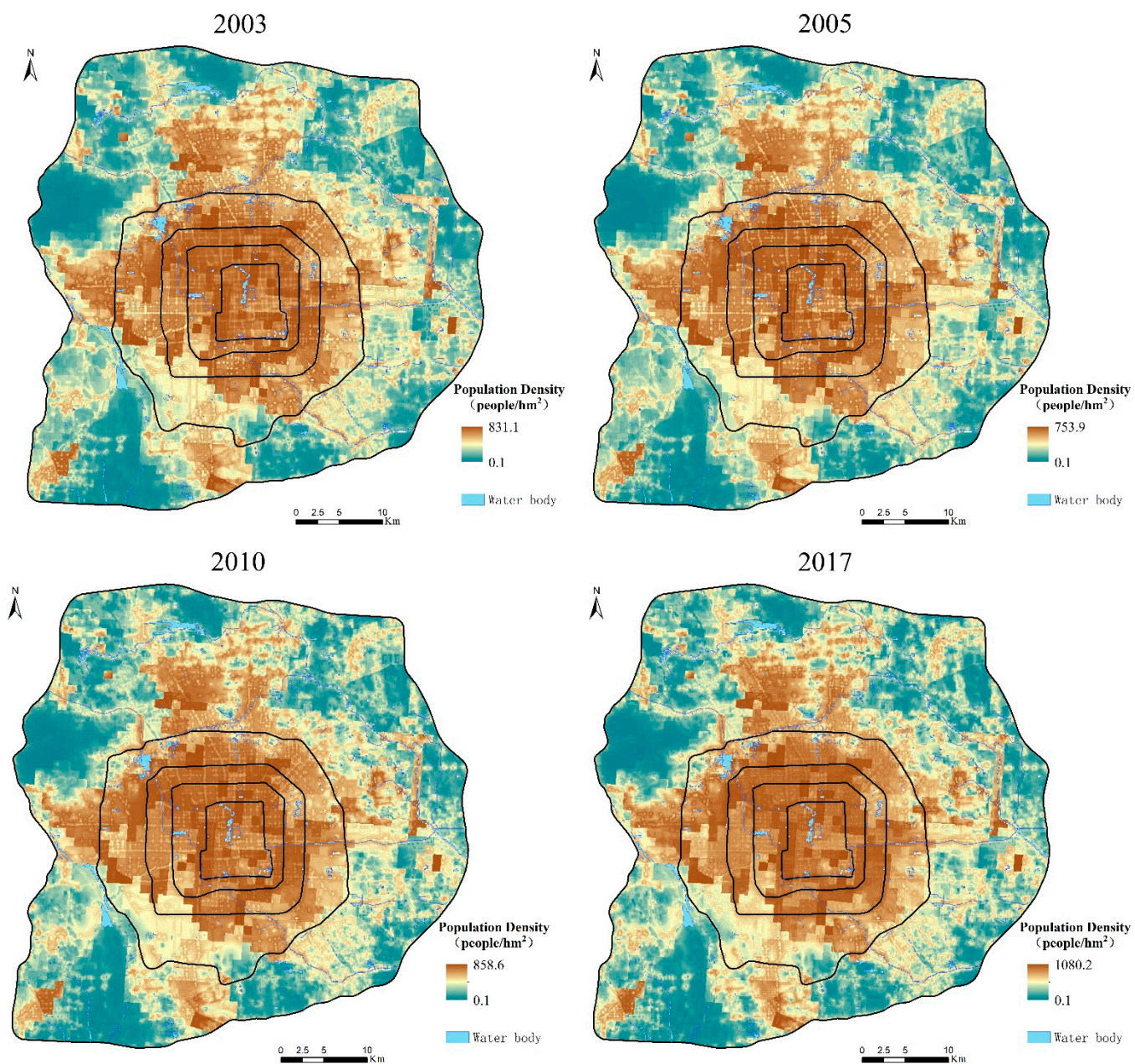


Figure S1. Population density distribution maps of 2003, 2005, 2010, and 2017

Reference

- Carlson, T.N., Ripley, D.A., 1997. On the relation between NDVI, fractional vegetation cover, and leaf area index. *Remote Sens Environ* 62, 241-252.
- Qin, Z., Li, W., Xu, B., Chen, Z., Liu, J., 2004. The estimation of land surface emissivity for Landsat TM6. *Remote Sensing for Land & Resources* 16, 28-32, 36, 41.
- Qin, Z., Li, W., Zhang, M., Karnieli, A., Berliner, P., 2003. Estimating of the essential atmospheric parameters of mono-window algorithm for land surface temperature retrieval from Landsat TM 6. *Remote Sensing for Land & Resources* 15, 37-43.
- Rozenstein, O., Qin, Z.H., Derimian, Y., Karnieli, A., 2014. Derivation of Land Surface Temperature for Landsat-8 TIRS Using a Split Window Algorithm (vol 14, pg 5768, 2014). *Sensors-Basel* 14, 11277-11277.
- Sobrino, J.A., Jimenez-Munoz, J.C., Paolini, L., 2004. Land surface temperature retrieval from LANDSAT TM 5. *Remote Sens Environ* 90, 434-440.
- Song, T., Duan, Z., Liu, J., Shi, J., Yan, F., Sheng, S., Huang, J., Wu, W., 2015. Comparison of four algorithms to retrieve land surface temperature using Landsat 8 satellite. *Yaogan Xuebao/Journal of Remote Sensing* 19, 451-464.
- Stewart, I.D., Oke, T.R., 2012. Local Climate Zones for Urban Temperature Studies. *B Am Meteorol Soc* 93, 1879-1900.
- Yang, J., Qiu, J., 1996. The Empirical Expressions of the Relation between Precipitable Water and Ground Water Vapor Pressure for Some Areas in China. *Scientia Atmospherica Sinica* 5, 620-626.